Japanese Journal of Applied Physics
Vol. 44, No. 1A, 2005, pp. 291–293

Liquid-Crystal-Based Fourier Optical Spectrum Analyzer without Moving Parts

Yan-qing LU, Fang DU, Yung-Hsun WU and Shin-Tson WU

College of Optics and Photonics/CREOL & FPCE, University of Central Florida, Orlando, Florida 32816, U.S.A.

(Received July 20, 2004; accepted October 4, 2004; published January 11, 2005)

We propose and demonstrate a liquid-crystal (LC)-based Fourier optical spectrum analyzer (FOSA). The FOSA consists of a birefringent filter array with an embedded LC phase modulator. The LC phase modulator is used to control the phase difference between two orthogonally polarized beams to avoid mechanical movement in conventional Fourier transform spectrometers. The detailed operation principle of this FOSA is described. A single-LC-based 6-stage FOSA is experimentally demonstrated, and the results obtained using such a FOSA show good agreement with the results measured using a reference spectrometer. [DOI: 10.1143/JJAP.44.291]

KEYWORDS: liquid crystal devices, Fourier transform spectrometer, Fourier series, dense wavelength-division multiplexing (DWDM), birefringent filter

1. Introduction

Fourier transform spectrometry (FTS) is one of the most powerful and popular methods available for various spectroscopy applications ranging from chemical analysis, environment monitoring and process control to astronomical observation.[1,2] FTS is generally performed using a Michelson interferometer, where light from a source is divided into two equal-intensity beams, with one of the beams traversing a variable light path. The two beams then recombine to generate optical interference. Normally, the variable light path is achieved by the mechanical movement of optical components. To ensure that the FTS system works, a fine and stable mechanical control is required. As a result, the final FTS system is bulky and expensive, and has a relatively slow operation speed.

It is highly desirable to develop a Fourier transform spectrometer without any mechanical moving parts so that it can be made more robust, compact and inexpensive. To date, several approaches generating a static phase (path) difference between two interference components have been proposed. For example, in a Wollaston prism with two wedges of a contiguously juxtaposed birefringent crystal or a liquid crystal (LC), a linearly varying phase shift is introduced between lights of different polarizations. Therefore, a light spectrum is obtained from the Fourier transform of the spatial intensity distribution.[3–5] Funk and Moore demonstrated solid-state FTS using prism pairs and a ferroelectric LC encoder array.[6] However, the Wollaston prism approach needs a precise image control and processing, and the LC array approach is complex. Recently, have we proposed a LC-based Fourier optical spectrum analyzer (FOSA) without moving parts.[7] The application of this device in dense wavelength-division multiplexing (DWDM) fiber-optic communication networks was emphasized.

In this study, we demonstrate a greatly improved system design of the LC-controlled FOSA. By using crystal quartz arrays and a single homogeneously aligned LC cell, a FOSA without moving parts was experimentally demonstrated. The results obtained using our FOSA agree well with those obtained using a reference spectrometer.

2. Mechanism

The LC FOSA that we previously proposed consists of a series of birefringent filters with different free spectral ranges (FSRs). Three control LC cells are employed in each FOSA stage to modulate the transmittance of each filter. Although the three-cell design provides the possibility of realizing a cascading one-dimensional system architecture, the precise control of these LC cells is complex and becomes more difficult in a multi-stage FOSA. To solve this problem, in this study, we demonstrate an improved and simplified design of a FOSA, as shown in Fig. 1. The new FOSA uses only one LC cell sandwiched between two crossed polarizers. The electronic control of the phase retardation of the cell is simplified considerably.

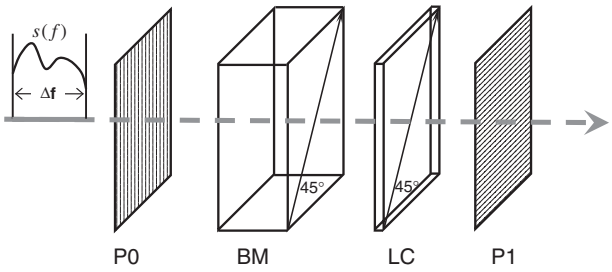

Fig. 1. Schematic diagram of single stage in LC-controlled FOSA. P0 and P1 denote crossed polarizers, and BM is a 45°-oriented birefringent material.

In Fig. 1, P0 and P1 are two crossed polarizers. Although parallel polarizers can also work, crossed polarizers are preferred because of their ease of alignment. BM represents a 45°-oriented birefringent material that could be a crystal or a liquid crystal. An electrically controlled homogeneous LC cell is placed behind the BM. Its optical axis is parallel to that of the BM, as shown in Fig. 1, so that the total phase retardation of BM and LC is additive. In such a FOSA stage, incoming light becomes linearly polarized after passing thorugh P0 and is decomposed into two equal orthogonally polarized components in BM and LC. These two polarization components recombine at P1 to generate optical interference. Obviously, this is a typical birefringent filter with a transmission of $T(f) = \sin^2[(\Gamma + \Gamma_{LC})/2] = (1/2)[1 - \cos(2\pi f/\mathrm{FSR} + \Gamma_{LC})]$,[8] where f is the light frequency, and $\Gamma = 2\pi f/\mathrm{FSR}$ and Γ_{LC} represent the phase retardation of the BM and LC cells, respectively. By tuning the applied voltage to the LC cell, LC directors are reoriented. As a result, Γ_{LC} changes and different transmission functions are obtained. For the FOSA application,

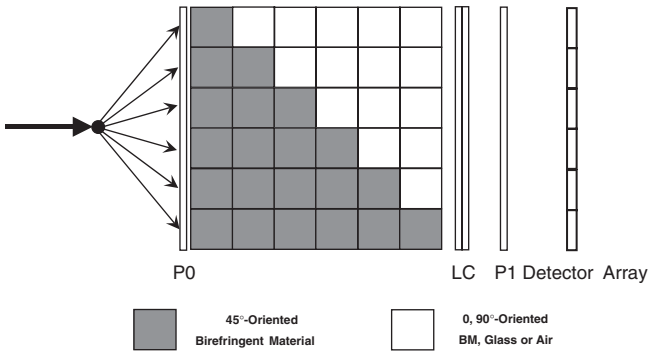

Fig. 2. System architecture of 6-stage LC-based FOSA.

the LC cell should be operated at 3 different retardation states, i.e., $\Gamma_{LC} = 2\pi$, $\pi/2$ and $3\pi/2$, at which the corresponding light transmittances are I_1, I_2, and I_3, respectively. It has been proven that the mth-order Fourier series coefficients of the input spectrum s(f) may be calculated from I_1, I_2, and I_3 by virtually expanding s(f) with a frequency period of $FP = m \cdot FSR$.[7)]

As a consequence, the input spectrum can be reproduced from its Fourier coefficients by employing sufficient stages with multiple FSRs. The whole FOSA system consists of a number of these stages that are packaged in parallel. Figure 2 shows the system architecture of such a FOSA. The input beam is separated into some channels with equal intensity by a $1 \times N$ polarization independent beam splitter, which is generally a planar-lightwave-circuit-based device. Each channel with a collimated input beam corresponds to a birefringent filter stage. The gray blocks represent the 45°-oriented birefringent materials, thus different stages will show different phase retardations. The white blocks could be 0° or 90°-oriented birefringent materials, optical glasses, or even just air which have no contribution to phase retardation. Because these birefringent filters are aligned parallel to each other, a single LC cell is sufficient for generating all the required phase states. Behind the polarizer P1, a photodetector array is placed to measure transmitted light intensity. Each detector pixel corresponds to a single FOSA channel so that an N-pixilated detector array is needed for an N-staged FOSA. Then the input spectrum can be reproduced with the Fourier coefficients computed from the detected light intensities in different pixels.

There are two key parameters for the LC-controlled FOSA: the maximum measurable spectral range and the minimum spectral resolution. Because the Fourier series only gives a periodic function, the maximum measurable spectral range is thus less than FP, which is just the FSR of the first FOSA stage. FSR is determined by material birefringence and thickness, thus, it should be carefully chosen to match a specific application. For example, for a telecom-based FOSA, the FSR should be wider than an International Telecommunication Union (ITU) spectral band with a width of 5 THz.

The spectral resolution of a spectrometer could be generally described as $|\delta f/f| = |\delta\lambda/\lambda| = \lambda/\Delta l$ regardless of spectrometer type, where δf and $\delta\lambda$ are the minimum distinguishable frequency and wavelength, respectively. Δl is the largest optical path difference between interfered lights. In a LC FOSA, Δl is the maximum optical retardation among all FOSA stages. Thus, the FOSA resolution can be derived as $\delta f = FP/N$. To increase spectral resolution, more FOSA stages have to be used. These stages may be aligned in a two-dimensional matrix to maintain a compact device footprint. However, in a fiber-optic communications system, all the light sources and amplifiers used have slowly varying spectral shapes, such as an erbium-doped fiber amplifier or a semiconductor amplifier. A low-resolution FOSA with less than 10 stages should be enough for telecom applications.[7)]

In addition to resolution, stage number N also affects the detected signal-to-noise ratio (SNR). The SNR is determined by the collected light intensity of each FOSA stage and the detector array's sensitivity. More stages may lower the SNR. A commercially available detector array has a responsivity of 0.95 A/W and a dark current of 0.03 nA. If only 1% power light is taped to a LC FOSA (<10 stages) for spectrum measurement, the total system light power should be higher than 0.063 mW to ensure SNR > 30 dB. Here, the 50% power loss of the polarizers has been taken into account. The actual transmitted light power in a DWDM system is at the milliwatt level, which indicates that the LC FOSA is sufficiently sensitive for practical applications.

3. Experimental Results

To prove the design principle, a prototype 6-stage FOSA device working at approximately $\lambda = 1.55\,\mu$m telecom band is experimentally demonstrated. Quartz crystals of 5 mm thickness are used as birefringent materials. The FSR for a single quartz crystal is calculated to be 7.1 THz in the near-infrared band. Although only one crystal is used for the first FOSA stage, the device dimension is determined by the sixth stage with 6 quartz crystals. An 8-μm-thick LC cell was used for the experiments. The inner surfaces of the substrates are coated with thin polyimide layers in antiparallel rubbing directions, which introduces a homogeneous alignment of LC molecules. Then the cell was filled with a Merck E44 LC mixture through a capillary effect. To determine the operating voltages of this LC cell, voltage-dependent transmittance was measured between the two crossed polarizers. Figure 3 shows the results. As the applied voltage increases, the transmitted light intensity oscillates. From Fig. 3, the

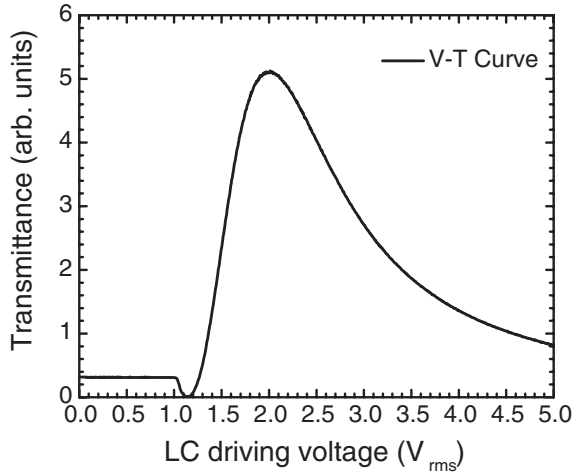

Fig. 3. Voltage-dependent transmittance of homogeneous E44 LC cell between two crossed polarizers. Cell gap $d = 8\,\mu$m, $\lambda = 1.55\,\mu$m, and $T = 22°$C.

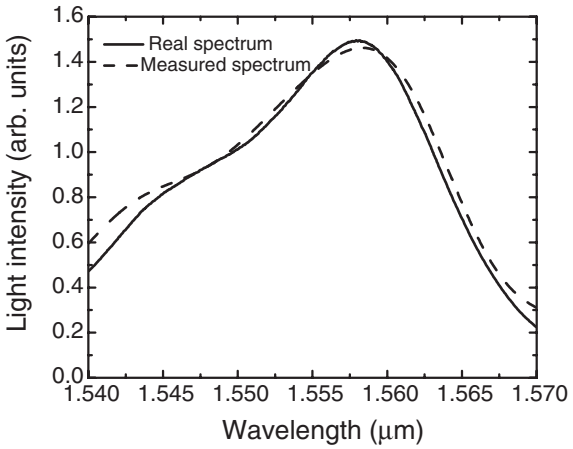

Fig. 4. Spectrum of broadband infrared source centered at $\lambda = 1.56\,\mu m$. The solid line is measured with a grating-based spectrometer, while the dashed curve is the spectrum reconstructed using the 6-stage FOSA.

voltage-dependent phase retardation can be calculated.[9] We found that the operating voltages corresponding to $\pi/2$, $3\pi/2$ and 2π phase retardations are 3.1, 1.5 and 1.1 V_{rms}, respectively. After installing the LC cell in the experimental setup, a computer-controlled LabVIEW system was used to drive the LC cell in the designed voltages sequentially and record the transmitted light intensity for each state. The input light spectrum is thus mathematically rebuilt from the calculated Fourier coefficients.

Figure 4 shows the spectrum of a broadband infrared-amplified spontaneous-emission light source centered at $\lambda = 1.56\,\mu m$. The dashed line is reconstructed from the measured Fourier coefficients with a 6-stage FOSA, while the solid line is the spectrum measured using a high-resolution grating-based spectrometer. The spectral curve measured using our FOSA matches the real spectrum reasonably well. The basic curve shape, peak position, and spectral width are all determined by the FOSA successfully. Several factors that were not considered in the calculation could have contributed to the observed experimental errors. For example, in our prototype FOSA, the phase retardation of each birefringent filter is quite large. The phase retardation of each filter may not be exactly multiple of that of the first stage due to the crystal misalignment and thickness variation, which may affect the final results.

Both our LC-controlled FOSA and the Wollaston-prism-based FTS[3–5] have no moving parts. However, the LC FOSA is Fourier-series-based while the latter is Fourier-transform-based. The LC FOSA is more suitable for digital control because it does not require any complex image processing. Their achievable resolution is comparable. The major difference is the maximum measurable spectral range. The LC FOSA only works in a designed spectral range but the FTS has no such limitation. The measurable spectral range of a FOSA can be widened by decreasing the phase retardation difference between adjacent stages but increasing the number of stages to keep the same resolution. The FOSA thus gradually becomes optically equivalent to a Wollaston-prism-based FTS with an embedded LC cell. In this case, both the "Wollaston prism" and LC cell can generate a variable phase difference. This hybrid FTS may have some special and interesting features that merit further studies. On the other hand, the LC used in the experiment is just a simple homogenously aligned cell. The transition time between different driving voltages is over 100 milliseconds, which is not very fast. To reduce response time, several approaches can be considered, for example, the use of a high figure-of-merit LC, the improvement of the driving scheme, and the introduction of polymer networks into LC.[10]

4. Conclusions

In summary, we experimentally demonstrated a 6-stage FOSA without moving parts. Unlike normal spectrometers, the FOSA retrieves the spectrum's Fourier coefficients instead of performs the direct spectrum measurement by controlling the phase retardation of a LC phase modulator. The measured spectrum of an infrared source shows a reasonably good agreement with the real spectrum. Some possible approaches to improving the FOSA performance are also discussed.

This work is supported by AFOSR under contract number F49620-01-1-0377.

1) A. Ben-David: Opt. Express **11** (2003) 418.
2) S. D. Collins, R. L. Smith, C. Gonzalez, K. P. Stewart, J. G. Hagopian and J. M. Sirota: Opt. Lett. **24** (1999) 844.
3) M. Francon and S. Mallick: *Polarization Interferometers* (Wiley, New York, 1971).
4) B. A. Patterson, M. Antoni, J. Courtial, A. J. Duncan, W. Sibbett and M. J. Padgett: Opt. Commun. **130** (1996) 1.
5) G. Boer, T. Scharf and R. Dandliker: Appl. Opt. **41** (2002) 1400.
6) D. J. Funk and D. S. Moore: Opt. Lett. **22** (1997) 1799.
7) Y. Q. Lu, C. Wong and S. T. Wu: IEEE Photonics Technol. Lett. **16** (2004) 861.
8) I. C. Khoo and S. T. Wu: *Optics and Nonlinear Optics of Liquid Crystals* (World Scientific, Singapore, 1993).
9) S. T. Wu, U. Efron and L. D. Hess: Appl. Opt. **23** (1984) 3911.
10) Y. Q. Lu, F. Du and S. T. Wu: Opt. Express **12** (2004) 1221.